Journal of Hydroscience and Hydraulic Engineering
Vol. 11, No. 2, January, 1994, 19-25

FRACTAL DIMENSION OF WATER PATH THROUGH UNSATURATED MEDIA AND ITS SIMULATION USING WATER PATH INVASION MODEL

BY

Yasushi Sakamoto
Associate Professor, Department of Civil and Environmental Engineering
Yamanashi University, Kofu, Japan

SYNOPSIS

Water flow path generated by micro-scale irregularity in uniformly-appearing unsaturated media was examined for its fractal dimension. This was done by experiments using the unsaturated media of glass-beads and by computer simulation using 'water path invasion model'.

Experimental water paths were visualized with colored water and their fractal dimensions were measured with the box-counting method. The experimental results showed that the water path develops a fractal pattern and its fractal dimension decreases as particle size increases.

Based on the experimental results, the 'water path invasion model' supposed that water selects its path according to the order of the possible flow rate resulting from the combined effects of capillary force, viscous force, and gravity. Computer simulation showed that the model can make the similar fractal water paths to the experimental ones, if it is supposed that relatively small pores can play no role for water path development.

INTRODUCTION

Water flow path plays a significant role for water and contaminants transport through unsaturated media. This water path is made mainly by macro-scale non-uniformity such as macro-pores or fissures in the media. But in some cases, the water path may be generated by micro-scale probabilistic irregularity such as pore size distribution even in uniformly-appearing unsaturated media. I investigated this type of water path on the basis of its fractal dimension by experiments using glass-bead layers and by computer simulation using 'water path invasion model' which involves the combined effects of capillary force, viscous force, and gravity.

FRACTAL DIMENSION OF WATER PATH THROUGH EXPERIMENTAL UNSATURATED MEDIA

Experimental Method

The experimental apparatus (as shown in Fig.1) consists of an acrylic box and a needle from which colored water drops onto the surface of an unsaturated medium. Initially, the bottom of the box was overlaid with big glass-beads (diameters of 4.0 mm and 2.8 mm) for drainage and the box was filled with water. Then glass-beads of several diameters was gradually put into the box and was compacted to make a stable layer of 76 cm depth. Finally, the water in the box was drained by gravity for about 30 minutes and the glass-bead layer was made to be a unsaturated medium. In this paper, the medium is treated as a two-dimensional field because the width of the medium surface is adequately small compared to its length.

The physical parameters of glass-bead layers are listed in Table 1. 'Mixture' in Table 1 means the mixture of glass-beads of two sizes. Mixture A consists of glass-beads of 1.41-1.71 mm and 0.84-1.00 mm diameter (ratio of average diameter =

1.69:1). Mixture B consists of glass-beads of 0.84-1.00 mm and 0.50-0.60 mm diameter (ratio of average diameter= 1.67:1). The ratio of numbers of big and small glass-beads is 5:2 for both mixture A and B. In this research, I assume that the experimental conditions made a statistically similar void space in each uniform glass-bead layer regardless of the difference in particle and pore sizes. For the mixtures, the similarity is supposed to be assured by setting the ratios of particle size and number in common between the two mixtures, A and B.

In Table 1, the parameters, b and ψ_e are the constants of water retention curves defined by the equation:

$$\psi = \psi_e (\theta/\theta_s)^{-b} \qquad (1)$$

where ψ = capillary potential; ψ_e = air entry potential; θ = unsaturated water content; θ_s = saturated water content; and b = a constant.

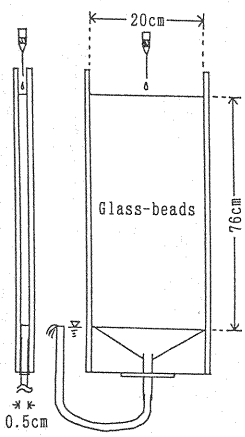

Fig.1 Experimental Apparatus

To make steady water paths, droplets of dilute NaCl solution were supplied onto the surface of the medium for about two hours at first. Then the water paths were visualized by tracer water colored with $KMnO_4$ of the same concentration as NaCl solution. Water supply rates were controlled by a micro-tube pump with a speed controller (Cole Parmer Instrument Co.). Water supply rates represented as intensity onto 20cm × 0.5cm surface were 45, 80, 150, and 200 mm/h. Resultant fractal patterns of water paths were recorded by photographs.

Table 1 Physical parameters of particle layers

Diameter (mm)	Porosity (%)	Darcy's k_s(cm/s)	Const. for Eq.1 ψ_e(cm)	b(-)
0.50-0.60	39.7	0.186	-14.5	0.23
0.71-0.84	39.3	0.304	-6.4	0.33
0.84-1.00	39.0	0.370	-5.3	0.38
1.00-1.41	40.2	0.536	-3.7	0.44
1.41-1.70	40.2	0.622	-2.8	0.47
Mixture A	38.7	0.595	-4.7	0.24
Mixture B	35.8	0.278	-7.0	0.25

Measurement of Fractal Dimensions of Water Paths

Fractal dimensions of water paths were measured by the box-counting method using the photographs. The pattern of water paths between 0 cm and 40 cm depths was covered with square boxes of size L × L and the number N(L) of boxes in which a part of water path exists were counted. If there is such relation between N(L) and L as presented below by Eq.2 , then D in Eq.2 is the fractal dimension:

$$N(L) \propto L^{-D} \qquad (2)$$

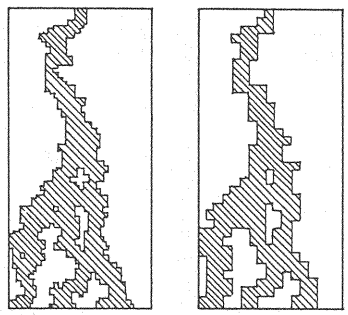

Fig.2 Boxes covering water path

The box size, L used for the experiments were 0.59, 1.18, 1.77, and 2.36 cm, which corresponds to 1, 2, 3, and 4 mm on 82 mm × 116 mm photographic prints, respectively. Fig.2 exhibits the example of water path covered with the boxes.

Experimental Results and Discussions

Fig.3 shows the example of water path observed in the experimental layers of glass-beads of : (a)small uniform diameter of 0.71-0.84mm, (b)big uniform diameter of 1.41-1.70 mm, (c)mixture A, and (d)mixture B. Fig.3 exhibits that the water path through a small particle medium

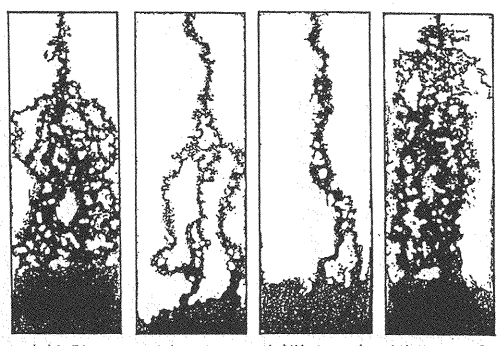

Fig.3 Examples of experimental water paths

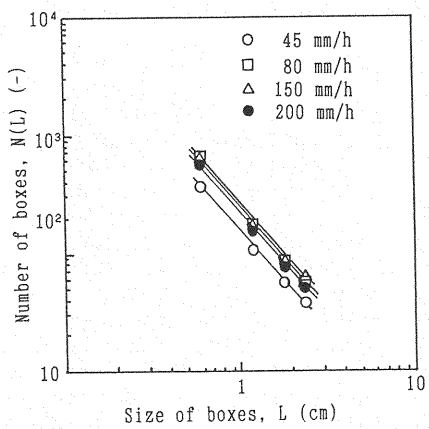

Fig.4 ln N(L) vs. ln L for experiments with several water supply rates

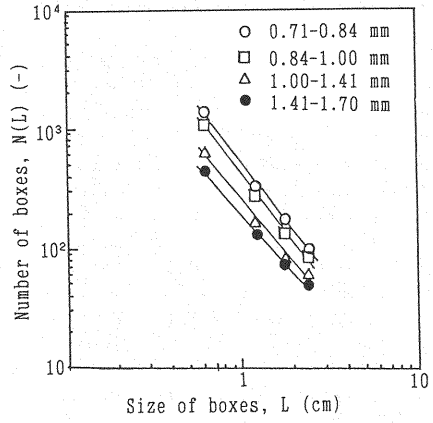

Fig.5 ln N(L) vs. ln L for experiments with several particle sizes

is more tortuous than one through a big particle medium. Figs. 4 and 5 shows the relation between ln L and ln N(L) for different water supply rates and for different particle size, respectively. These figures shows that ln L and ln N(L) are linearly related to each other for every case and that the water paths are fractal. We can also find that the fractal dimension does not depend on the water supply rate, but considerably depends on the particle size.

The relation between the average diameter of particles and the fractal dimension is shown in Fig.6. In Fig.6, triangles and squares represent the average diameters of small and big particles in mixture A and B. Fig.6 shows that the fractal dimension of water path for uniform-diameter particles decreases as the particle size increases and that the fractal dimension for the mixtures is more strongly influenced by the size of small particles than by that of bigger ones.

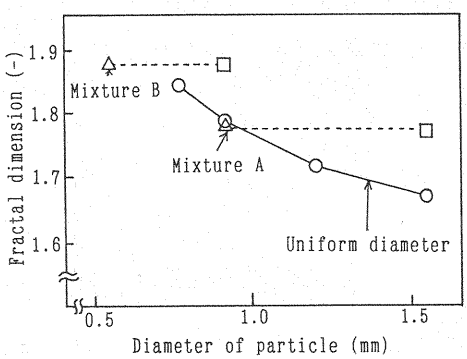

Fig.6 Fractal dimension of water path vs. diameter of particle for experiments

If only capillary force is dominant for water path formation, the resultant water paths through the media with similar void space are expected to be statistically similar regardless of the difference in particle and pore sizes. This expectation is based on the principle of the invasion percolation model which will be explained later. The experimental results shows that the similar void space can produce the water paths of different fractal dimensions, if the particle and pore sizes are different. This result suggests that there are other factors such as gravity that are also dominant for water path formation.

FRACTAL DIMENSION OF WATER PATH PRODUCED BY COMPUTER SIMULATION

Water Path Invasion Model

In this paper, I propose the 'water path invasion model'. This model is named after the 'invasion percolation model' that has been proposed for capillary displacement in porous media (1,2,5). At first, the 'invasion percolation model' will be discussed.

Lenormand et al. (2,3) have presented a phase diagram for two-dimensional immiscible displacements in porous media, and have classified those displacements to three categories characterized by two dimensionless numbers; the capillary number and the ratio of the viscosities of two fluids. The three categories are:

(a) capillary fingering when capillary forces are very strong compared to viscous force;
(b) viscous fingering when a less viscous fluid is displacing a more viscous one;
(c) stable displacement in the opposite case.

The invasion percolation model have been presented to describe the capillary fingering. In this model, a porous medium is represented as a finite two-dimensional network (or lattice) of pores (located on the sites or nodes) and throats (on the bond or links). The fluid motion through the medium is represented as a stepwise Monte Carlo process on the lattice, where at each step the fluid interface moves through the lattice link where the displacing force is largest. In this model, the only displacing force is the capillary force, and inertial and gravity effects are supposed to be negligible. In this model, the order of displacing force of each link determines the order of pores to be displaced. Therefore the simulation can be performed only if the order is given for links, and the size of each link has nonsense. The experimental results mentioned above shows the effect of the size on the fractal dimension of water path for the similar void space. I thought this contradiction is due to the gravity effect and revised the invasion percolation model to make the 'water path invasion model' that applies the combined force of gravity and capillary force to the displacing force.

The 'water path invasion model' supposes that the driving forces for displacement are capillary force and gravity, and that the flow through each link is a Poiseuille flow. The direction of the links is set to be horizontal or vertical. In this model, which node (or pore) is to be displaced at next step is determined by comparing the possible flow rate of each link (or throat) contacted with the interface between water and air. The possible flow rate, q is defined for horizontal and vertical links by:

$$\text{horizontal:} \quad q = F1 \tag{3}$$

$$\text{vertical(downward):} \quad q = F1 + F2 \tag{4}$$

$$\text{verical(upward):} \quad q = F1 - F2 \tag{5}$$

using

$$F1 = (\pi 2\gamma\cos\alpha/8\mu)\, a^3/l \tag{6}$$

$$F2 = (\rho g\pi/8\mu)\, a^4 h/l \tag{7}$$

where a = the diameter of link (or throat); l = length of link; h = the difference in hydraulic head between the both ends of link; ρ = the density; μ = the viscosity; γ = the surface tension; α = the contact angle; and g = the gravitational acceleration.

F1 and F2 represent the contribution coefficients of capillary force and gravity to the possible flow rate, respectively. By supposing that h = 1 and putting the values of physical characteristics of water (i.e. γ = 0.072752 kg/sec^2, α = 9° etc.) into the constants in Eqs. 6 and 7, the contributions of capillary force and gravity can be summarized as:

$$f1 = a^3/l \tag{8}$$

$$f2 = 68.2\times10^3\times a^4 \tag{9}$$

where f1, f2 = the contribution indices (in units of 1/m^2) of capillary force and gravity for water flow, respectively.

Table 2 Simulation conditions

	d=2r (mm)	a/r (-)	l/r (-)	Comments
Case A1.1	1.56	0.155-1.000	1.15-3.46	
Case A1.2	1.56	0.414-1.000	2.00-3.46	
Case A1.3	1.56	0.707-1.000	2.73-3.46	
Case A1.4	1.56	0.800-1.000	3.00-3.50	
Case A2	1.56	0.707-1.000	2.73-3.46	No Trap
Case A3	1.56	0.707-1.000	2.73-3.46	No Gravity
Case A4	1.56	0.285-1.000	1.58-3.46	Vertical
(Anisotropy)		0.155-0.707	1.15-2.73	Horizontal
Case B	1.21	0.707-1.000	2.73-3.46	
Case C	0.92	0.707-1.000	2.73-3.46	6000 Steps

Simulation Conditions

To calculate the indices, f1 and f2

for each link, the ratios of a and l to particle radius, r for each link were assigned within the range shown in Table 2. The minimum and maximum values of the range in Table 2 are originated from the values for such regular arrangements as simple rhombic layer (a/r=0.155, 1/r=1.15), square layer (a/r=0.414, 1/r=2.0), and simple rhombic layer with pores of particle size (a/r=1.0, 1/r=3.46). The values of a/r and 1/r for each link were determined in the range by using the {0,1} uniform-distribution random numbers generated by computer. Because a/r and 1/r of each link were determined by using the same random number, the link of small diameter was assigned with more short length than that of big diameter.

The number of nodes, n, for the particles of diameter d was set to be 100/d for horizontal direction and 2.5 × n for vertical direction. The boundary condition for side walls was set to be closed. The simulations were ended when the front of the displacing water reached the lowest line of nodes except for Case D, where the simulation was ended at 6,000 steps (the CPU time was 4 hours and 10 minutes by 24.0 MIPS computer). The effect of entrapped air was also introduced by preventing the water path from invading into the trapped air area.

Some special conditions such as no trapping (Case A2), no gravity (Case A3), and anisotropy (Case A4) were also examined. The anisotropy was simulated by using the different ranges of a/r and 1/r for the horizontal and vertical directions. For Case A1.1-A1.4, two or three random number series were used and the averaged fractal dimension was determined. For other cases, only one series was used.

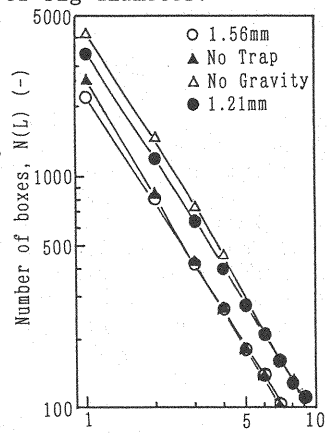

Fig.7 ln N(L) vs. ln L for simulations

Simulation Results and Comparison with Experimental Results

Fig.7 shows relation between ln N(L) and ln L. Here L is represented by the number of nodes. The area for box-counting was limited to the upper 2 × n lines to eliminate some outlet effects. Fig.7 shows that there is a linear relation between ln L and ln N(L) when L is bigger than 3. Therefore, the fractal dimension for each case was calculated using data of r > 3.

The examples of simulated water paths are shown for the same series of random numbers in Fig.8. In Fig.8, (a) is the case with air-trapping and gravity effect, (b) is without air-trapping effect but with gravity effect, and (c) is without both air-trapping and gravity effects. The fractal dimensions are 1.63 for (a), 1.67 for (b), and 1.73 for (c). These figures show that the air-trapping does not have a significant effect on the shape of the water path, and that gravity restrains the water path expansion toward the lateral direction. The fractal dimension for the case without gravity is significantly bigger than those of the experimental results. This suggests the important role of gravity for water path formation.

The relation between a/r and the

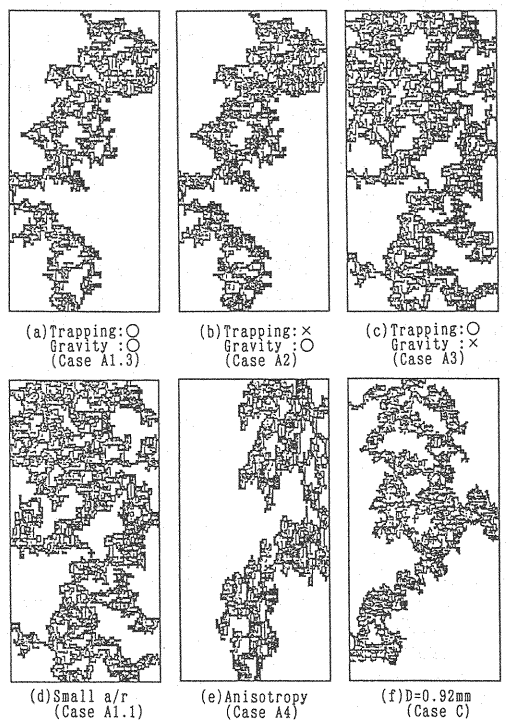

Fig.8 Examples of simulated water paths

fractal dimension is shown for 1.56 mm particles in Fig.9. Fig.9 shows that if there are relatively small links, the fractal dimension is bigger than those observed at the experiments. The water path for this case is shown in Fig.8 (d). This figure is very similar to that for no gravity shown in Fig.8 (c). The results of the simulations suggest that the relatively small link does not play a significant role for actual water path formation.

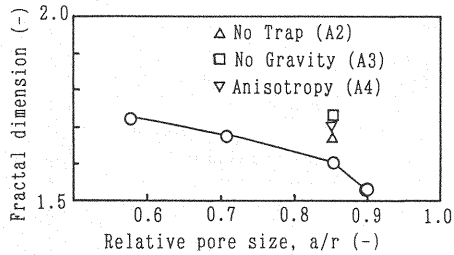

Fig.9 Fractal dimension of water path vs. relative pore size for simulations

The anisotropy in the simulations made the trapped-air zone lengthened toward longitudinal direction as shown in Fig.8 (e). The trapped-air zones of experiments were not similar to those of simulations. Therefore the experimental conditions make no significant effect of anisotropy.

The water path for small particles is shown in Fig.8 (f) which is the result of simulation with 0.92 mm particle at 6,000 steps. The fractal dimension of this case is 1.71 which is bigger than 1.61 for 1.56 mm, while the fractal dimension for 1.21 mm (Case B) is 1.60 which is almost same as for 1.56 mm. This suggests that the model can make similar relation between the fractal dimensions and the pore sizes to that of the experiments as shown in Fig.6.

CONCLUSIONS

In this paper, I examined the fractal dimension of water path through uniformly-appearing unsaturated media by the experiments using glass-bead layers and the simulation using 'water path invasion model'. The model supposes that the water path invades the easiest link to go into on the basis of possible flow rate derived by gravity and capillary force. The conclusions of this paper are listed below.

For the experiments:

(1)The water paths through unsaturated glass-bead layers are fractal.

(2)The fractal dimension of the water path is not significantly influenced by flow rates, but significantly influenced by particle size.

(3)The fractal dimension decreases as particle size increases. The fractal dimension for the mixture of two size glass-beads is more influenced by the size of small particle.

These results indicates the contribution of gravity.

For the simulations:

(4)Water path invasion model can make the water path of similar fractal dimension to that of experiments if it is supposed that the relatively small pore plays no significant role for actual water path formation.

(5)The model can also simulate the effect of pore size on the dimensions.

ACKNOWLEGEMENT

This research was supported in its experimental part by Mr. H. Shibata who is a graduated student of our department.

REFERENCES

1. Chandler, R., J.Koplic, K.Lerman and J.F.Willemsen : Capillary displacement and percolation in porous media, J. Fluid Mech., Vol.119, pp.249-267, 1982.
2. Lenormand, R., E.Touboul and C.Zarcone : Numerical models and experiments on immiscible displacement in porous media, J. Fluid Mech., Vol.189, pp.165-187, 1988.
3. Lenormand, R. : Flow through porous media: limits of fractal patterns, Proc. R. Soc. London, A423, pp.159-168, 1989.
4. Lenormand, R. : Capillary Fingering: Percolation and Fractal Dimension, Transport in Porous Media, 4, pp.599-612, 1989.

5. Wilkinson, D. and F.Willemsen : Invasion percolation: a new form of percolation theory, J. Phys. A:Math/ Gen., 16, pp.3365-3376, 1983.

APPENDIX-NOTATION

The following symbols are used in this paper:

- a = diameter of link;
- b = constant of water retention curve;
- d = particle diameter;
- D = fractal dimension of water path;
- $f1$ = contribution index of capillary force to water flow;
- $f2$ = contribution index of gravity to water flow;
- $F1$ = contribution coefficient of capillary force to possible flow rate, q;
- $F2$ = contribution coefficient of gravity to possible flow rate, q;
- g = gravitational acceleration;
- h = difference in hydraulic head between both ends of link;
- k_s = hydraulic conductivity of a saturated medium;
- l = length of link;
- L = size of box used for box-counting method;
- n = pore number in one line which was used by simulation;
- $N(L)$ = number of L-size boxes which cover the water path;
- q = possible flow rate through link;
- α = contact angle;
- γ = surface tension;
- θ = unsaturated water content;
- θ_s = saturated water content;
- μ = viscosity;
- π = 3.14159....;
- ρ = density;
- ψ = capillary potential; and
- ψ_e = air entry potential, respectively.

(Received November 18, 1992: revised June 9, 1993)